Acta Pharmaceutica Sinica B 2020;10(1):79–90

Chinese Pharmaceutical Association
Institute of Materia Medica, Chinese Academy of Medical Sciences

Acta Pharmaceutica Sinica B

www.elsevier.com/locate/apsb
www.sciencedirect.com

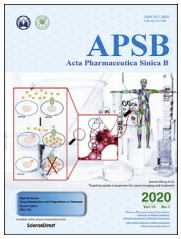

REVIEW

Targeting uptake transporters for cancer imaging and treatment

Yuchen Zhang, Joanne Wang*

Department of Pharmaceutics, University of Washington, Seattle, WA 98195, USA

Received 28 June 2019; received in revised form 27 September 2019; accepted 17 November 2019

KEY WORDS

Uptake transporter;
Warburg effect;
Cancer imaging;
Neuroblastoma;
Thyroid cancer;
mIBG

Abstract Cancer cells reprogram their gene expression to promote growth, survival, proliferation, and invasiveness. The unique expression of certain uptake transporters in cancers and their innate function to concentrate small molecular substrates in cells make them ideal targets for selective delivering imaging and therapeutic agents into cancer cells. In this review, we focus on several solute carrier (SLC) transporters known to be involved in transporting clinically used radiopharmaceutical agents into cancer cells, including the sodium/iodine symporter (NIS), norepinephrine transporter (NET), glucose transporter 1 (GLUT1), and monocarboxylate transporters (MCTs). The molecular and functional characteristics of these transporters are reviewed with special emphasis on their specific expressions in cancers and interaction with imaging or theranostic agents [*e.g.*, I-123, I-131, ^{123}I-iobenguane (mIBG), ^{18}F-fluorodeoxyglucose (^{18}F-FDG) and ^{13}C pyruvate]. Current clinical applications and research areas of these transporters in cancer diagnosis and treatment are discussed. Finally, we offer our views on emerging opportunities and challenges in targeting transporters for cancer imaging and treatment. By analyzing the few clinically successful examples, we hope much interest can be garnered in cancer research towards uptake transporters and their potential applications in cancer diagnosis and treatment.

Abbreviations: CT, computed tomography; DDI, drug–drug interaction; DTC, differentiated thyroid cancer; FDA, U.S. Food and Drug Administrations; FDG, fluorodeoxyglucose; GLUT, glucose transporter; IAEA, the International Atomic Energy Agency; LACC, locally advanced cervical cancer; LAT, large amino acid transporter; MCT, monocarboxylate transporter; mIBG, iobenguane/meta-iodobenzylguanidine; MRI, magnetic resonance imaging; NE, norepinephrine; NET, norepinephrine transporter; NIS, sodium/iodine symporter; OCT, organic cation transporter; PET, positron emission tomography; PHEO, pheochromocytoma; RA, retinoic acid; RET, rearranged during transfection; SLC, solute carrier; SPECT, single-photon emission computed tomography; SUV, standardized uptake value; TFB, tetrafluoroborate; TSH, thyroid stimulating hormones; vHL, von Hippel-Lindau.

*Corresponding author. Tel.: +1 206 2216561; fax: +1 206 5433204.
E-mail address: jowang@uw.edu (Joanne Wang).

Peer review under responsibility of Institute of Materia Medica, Chinese Academy of Medical Sciences and Chinese Pharmaceutical Association.

https://doi.org/10.1016/j.apsb.2019.12.005

1. Introduction

Detection and localization of tumor is the first and essential step for any cancer therapy for solid tumors. More importantly, the early detection of tumor is the key to improve the survival rate for many different types of cancers[1]. Cancer imaging is the most widely applied non-invasive method for the detection of tumors. Besides detection, cancer imaging is also used for the staging and monitoring of therapeutic response in certain cancers[2]. Currently, several major imaging modalities are available, including X-ray [plain film and computed tomography (CT)], ultrasound, magnetic resonance imaging (MRI), single-photon emission computed tomography (SPECT), positron emission tomography (PET) and optical imaging[3]. Besides non-invasiveness, low-to-none tissue destruction, with the improvement of radiotracer, some of the modalities can also track the cell metabolism and tissue environment changes *in vivo*[4]. However, one of the major challenges for cancer imaging is sensitivity and specificity[2]. The threshold for conventional anatomic imaging modalities (*e.g.*, CT, MRI and ultrasound) to detect a tumor lesion is around 1 cm^3, or roughly $\sim 10^8$ cells for tumors with epithelial origin, which essentially means that a patient with negative imaging results could still have as many as 10^8 tumor cells in the body[2,5]. Newer molecular imaging approaches designed to target tumor-specific biomarkers or proteins with enriched expression and activity in cancer cells are expected to have a major impact on cancer detection and treatment[6].

Solute carrier (SLC) transporters are a major type of membrane transport proteins that transport nutrients, neurotransmitters, hormones, drugs, and toxins across cell membranes. Currently, more than 400 SLC members have been identified in the human genome. Primarily involved in the uptake of small molecules into cells, these transporters play important roles in physiological and pharmacological processes, such as cellular uptake of nutrients and metabolites, clearance of released neurotransmitters, and absorption, distribution and excretion of drugs and other xenobiotics[7]. In the past few decades, fueled by molecular cloning and functional characterization of various transporters, great progress has been made in our understanding of the roles of uptake transporters in drug disposition, drug−drug interactions (DDIs), drug efficacy and toxicity[8]. Grounded in these research findings, the U.S. Food and Drug Administrations (FDA) has developed recommendations for pharmaceutical industry to evaluate transporter-mediated DDIs during drug development[9].

In the imaging field, uptake transporters are of great interest owing to their natural ability to concentrate endogenous compounds or xenobiotics into cells. Combined with increased knowledge in transporter expression in specific tissue or cell type, targeting an uptake transporter with an appropriately labeled substrate could be used for tissue specific imaging *in vivo*[7,10]. An effective radiotracer can also be further developed into a therapeutic agent by replacing the radioisotope to another one with stronger α- or β-emissions[11]. When a single agent is used to simultaneously or sequentially diagnose and treat medical conditions, it becomes a "theranostic" agent, a term derived from a combination of the words "therapeutics" and "diagnostics". Transporter-based "theranostics" are especially appealing in the context of cancer as certainly uptake transporters are uniquely expressed or enriched in cancer cells due to the unique lineage and/or abnormal demands of tumor cells for nutrients and hormones as compared to normal cells.

Compared to the vast research on transporters' roles and impacts on drug disposition, pharmacokinetics and DDIs, much less attention has been given to the specific expression of uptake transporters in cancer cells and their potentials for developing new agents for cancer diagnosis and treatment. On the other hand, a number of clinically important imaging agents (Fig. 1), such as ^{18}F-fluorodeoxyglucose (^{18}F-FDG), radioiodine and ^{123}I-iobenguane (mIBG), were developed based on enhanced uptake in cancer cells long before the underlying transporters were cloned and characterized at the molecular level. In this article, we focus on several SLC transporters responsible for transporting clinically used imaging agents into cancer cells including the sodium/iodine symporter (NIS), the norepinephrine transporter (NET), glucose transporters (GLUTs) and monocarboxylate transporters (MCTs, Table 1). The molecular characteristics, substrate specificity, transport modes, tissue distribution and physiological function of these transporters will be reviewed in the context of clinical background. The expression of these transporters in cancer cells and their specific interaction with the imaging agents will be highlighted. Current clinical and research areas of these transporters in cancer diagnosis and treatment will be discussed. Finally, we offer our views on emerging opportunities and challenges in targeting transporters for cancer imaging and treatment.

2. NIS and thyroid cancer imaging

2.1. *Clinical background*

The therapeutic use of I-131 in thyroid cancer is the cornerstone of nuclear medicine. In the early 1940s, it has already been applied for the treatment of both hyperthyroidism and thyroid cancer, which eventually lead to the approval of medical radioisotope use and foundation of nuclear medicine[12]. During the past 50 years, radioiodine was widely used for the diagnosis and treatment for thyroid cancer and its metastasis based on the observation that iodine can be concentrated in cancer cells. However, it was until 1996 the transporter for iodine uptake in thyroid follicle cells was first cloned and named as sodium/iodine symporter (NIS)[13].

2.2. *Molecular and physiological characteristics of NIS*

NIS, encoded by *SLC5A5*, belongs to *SLC5* family. The glycoprotein contains 643 amino acids with an apparent molecular weight of 70−90 kDa[14]. NIS transports two sodium ions with one iodide ion by utilizing the physiologic transmembrane sodium gradient as the energy source. This ion exchange process can lead to the accumulation of iodide ion in thyroid by a factor of 20−40 times[15]. Under physiological condition, iodide ions target NIS to entry the thyroid follicle cells and then are pumped into the colloid by pendrin for further organification into T_3 and T_4[15]. Besides transporting I^- at a K_m value of $\sim$20 μmol/L, NIS can also facilitate the uptake of other anions including thiocyanate, chlorate, perrhenate and perchlorate. Interestingly, the entry of perrhenate and environmental pollutant perchlorate can be transport into thyroid gland with an electroneutral stoichiometry (one Na^+/one anion), while most other anions follow 2:1 ratio[16]. The function and expression of NIS in thyroid follicle cells can be highly modulated by its primary modulator thyroid stimulating hormones (TSH) though cAMP signal transduction pathway[17]. Another major modulator of NIS is its substrate I^-. The accumulation of I^- intracellularly can destabilize NIS mRNA, which slow down the further accumulation, prevent the production of reactive oxygen species and toxicity by high I^- concentration in thyroid.

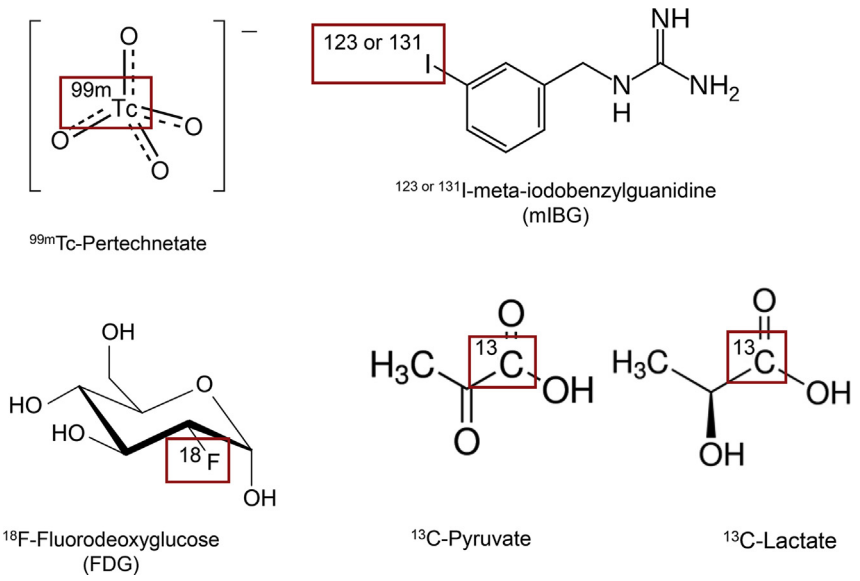

Figure 1 Chemical structures of selected cancer imaging and theranostic agents. Boxed region indicates position for radioisotope labeling.

Besides thyroid follicle cells, moderate NIS protein expression can also be found in salivary gland[18] and lactating breast[19]. In salivary glands, NIS is mainly expressed at the basolateral plasma membrane of epithelial ductal cells and facilitate the uptake of I^-, and the function of NIS is considered as a mechanism to protect and heal antimicrobial function[20]. In breast, NIS only expresses when late in pregnancy and during lactation, while ovariectomized animal models demonstrated that the overexpression of NIS in mammary glands is mediated by oxytocin, estradiol and prolactin[19].

2.3. *Expression of NIS in thyroid and breast cancer*

In cancers, the protein expression of NIS can be detected in only thyroid cancer and breast cancer[15]. Thyroid cancer has a relatively low prevalence (0.74% in men and 2.3% in women), and a favorable prognosis due to the effectiveness of surgical therapy followed by radioablation[15]. The efficacy of radiotherapy is highly dependent on the selective NIS expression, and with more than 70% of differentiated thyroid cancers (DTC) expressing NIS, the response rate is relatively high for radioablation[11]. Unfortunately,

Table 1 Selected transporters involved in cancer imaging and therapy.

Transporter	NIS	NET	GLUT1	MCT1 and MCT4
Gene	*SLC5A5*	*SLC6A2*	*SLC2A1*	*SLC16A1* and *SLC16A3*
Physiological substrate	I^- SCN^-	Norepinephrine Dopamine Serotonin	Glucose Mannose Galactose Glucosamine	Lactate Pyruvate
Expression in cancer	Thyroid Breast	Neuroblastoma Pheochromocytoma	Widely expressed in different cancers including pancreas, breast, lymphomas, prostate, head and neck cancer.	Widely expressed in different cancers including head and neck, breast, lung, bladder, prostate, and glioma.
Agents in development	Diagnosis: ^{18}F tetrafluorobrate Therapy: Re-186 Re-188 At-211	Diagnosis: ^{18}F-MFBG ^{11}C-HED ^{18}F-FDA ^{18}F-DOPA Therapy: ^{211}At-MABG	Diagnosis: 6-^{18}F-FDF 1-^{18}F-FDAM	Diagnosis: hyperpolarized ^{13}C glucose ^{13}C lactate ^{13}C pyruvate
Agents approved for clinical use	Diagnosis: I-123 I-124 ^{99m}Tc pertechnetate Therapy: I-131	Diagnosis: ^{123}I-mIBG Therapy: ^{131}I-mIBG	Diagnosis: ^{18}F-FDG	Under development

dedifferentiated thyroid cancer and metastasis thyroid cancer has a lower and/or internalized expression of NIS, which significantly reduced the efficacy of radiotherapy[21,22]. Side effect caused by radiotherapy for thyroid cancer is common (10%−60%) but moderate, because of the relatively lower expression of NIS in other tissues[23]. Besides thyroid cancer, around 80% of breast cancers show high NIS expression. More importantly, a clinical study showed positive immunohistochemistry staining of 86% of 49 invasive breast cancer or ductal carcinoma patients, while only 23% of 13 extratumoral samples from the vicinity of the tumors[19]. This relatively high expression selectivity makes NIS a potential target for breast cancer.

2.4. *Radioisotope imaging agents for NIS*

For diagnosis, I-131 was first used in DTC since more than 70 years ago. With the improvement of technology, both I-123 and I-131 were used for gamma scan. As a proton enriched isotope of iodine, I-124 can also be used in PET and lead to a better sensitivity[24]. However, the β energy of I-131 is relatively high for imaging use and can lead to potential radiotoxicities. On the other hand, both I-123 and I-124 need to be generated by cyclotron, which is not readily available and more expensive. Hence, additional imaging tools are being developed to target NIS in DTC[25]. ^{99m}Tc pertechnetate (Fig. 1) was identified as a substrate of NIS in both *in vitro* and *in vivo* system[26,27]. To our knowledge, no K_m data is available for ^{99m}Tc pertechnetate. However, the affinity of ^{99m}Tc pertechnetate towards NIS was estimated to be higher than I^- based on indirect *in vitro* and *in vivo* evidences[28−30]. ^{99m}Tc pertechnetate also emits no β ray but 140 keV gamma ray, which is the ideal peak for gamma camera imaging. Besides its advantage in the physiochemical properties, ^{99m}Tc pertechnetate is relatively low in production cost and more available in clinical setting. These characteristics has made ^{99m}Tc pertechnetate one of the most widely used reagent for routine DTC imaging[25]. Recently, F-18 labeled tetrafluoroborate (^{18}F-TFB) was also synthesized and identified as a NIS specific substrate[31]. *In vivo* biodistribution study and PET scanning showed that 60 min after injection, more than 90% of the ^{18}F-TFB signals can be obtained from thyroid or thyroid tumors, indicating that ^{18}F-TFB can be rapidly concentrated into NIS-expressing tissues and be used as a potential diagnostic tool[31]. Currently, a clinical study is ongoing at the Memorial Sloan Kettering Cancer Center (New York, NY, USA) to evaluate the use of ^{18}F-TFB in thyroid cancer patients (NCT03196518).

2.5. *NIS-based approach to improve cancer targeting*

Several other radioisotopes which can emit particles have been identified as the substrate of NIS and can be developed into new radiotherapies, such as Re-188, Re-186 and At-211[22]. However, I-131 remains the most preferred radioisotope for thyroid cancer because after the uptake through NIS, thyroid follicle cells can trap I-131 by organification of I-131 into T_3 and T_4[15]. The long retention of I-131 in thyroid cancer provides a therapeutic advantage to destroy tumor cells with β particles.

As the major target for the diagnosis and therapy of thyroid cancer, the expression of NIS is crucial for prognosis. Several studies have proven that the NIS protein expression is correlated with I-131 uptake[32,33] and thyroid cancer prognosis[34]. Thus, the modulation or increase of NIS expression could be beneficial for the NIS-mediated imaging and therapy. A number of studies have been conducted to investigate potential methods to increase NIS expression in cancer cells. Activation of TSH is one of the most well studied methods to increase NIS expression. Studies have shown that TSH can increase both mRNA and protein expression in thyroid cancer cell lines[17,35], and also post-translationally modify NIS which increases its membrane expression[36]. The administration of recombinant TSH (thyrogen) or withdrawal of thyroid hormone supplement after thyroidectomy has already been used in patients to elevate serum TSH level and lead to an induction of NIS expression[37]. In breast cancer, retinoic acid (RA) is the most potent single-agent NIS inducer[38]; however, RA cannot induce NIS in thyroid cancer but reduce its expression[39]. Several other NIS modulation agents and transcriptional factors have been identified in the last decade, and been well summarized in a recent review[11].

2.6. *NIS-based gene therapy for non-thyroid cancers*

NIS-mediated uptake of radioisotope showed convincing success in the theranosis of DTC; however, this line of nuclear medicine showed lower response rate for tumors with lower or no expression of NIS[22]. Radionuclide gene therapy using NIS was then proposed to solve this problem, and potentially apply to other non-thyroid cancers (Fig. 2). Several studies have shown that after transfected with NIS in different cancers, the radioiodine uptake into tumors significantly increased and could be used for imaging and radiotherapy[40]. For example, the Morris group constructed an adenovirus containing MUC1 promoter and NIS gene, and successfully infected MUC1-positive pancreatic-tumor xenografted mouse with this construct. After infection, the uptake of radioiodine can be observed under gamma camera in the transduced tumor[41]. However, one major concern for the application of this gene therapy is that unlike thyroid cancer, radioiodine cannot be organified in other tumors, and thus the retention time may not be long enough for the β particles to destroy the cancer cells. The co-transfection of NIS and thyroid peroxidase gene was purposed to solve this problem but the results were not effective[40].

Over the last century, the theranostic use of NIS-mediated radioisotope uptake pathway has been identified, characterized and widely applied in thyroid cancers and potentially other cancers. With the fast advancement of molecular imaging and gene therapy, radioisotopes targeting NIS with higher resolution could be expected and clinical application of NIS-mediated radiotherapy in other cancers are likely to be seen in the near future.

3. Norepinephrine transporter and neuroblastoma

3.1. *Clinical background*

Neuroblastoma is the most common extracranial solid tumor in children accounting for 15% of deaths from all pediatric cancers [42-45]. Neuroblastoma is originated from the neural crest cells of the sympathetic nervous system; and most neuroblastoma cells are positive for cell surface expression of the NET[46−48]. *Meta*-iodobenzylguanidine (mIBG, Fig. 1), also known as iobenguane, is a structural analog of norepinephrine (NE), the natural substrate of NET. mIBG was first developed to image adrenal medulla as a scintigraphic tool in 1980s[49]. When radio-labeled with the gamma-emitter I-123, ^{123}I-mIBG can be effectively used in whole body imaging of neuroblastoma. ^{123}I-mIBG has superior image

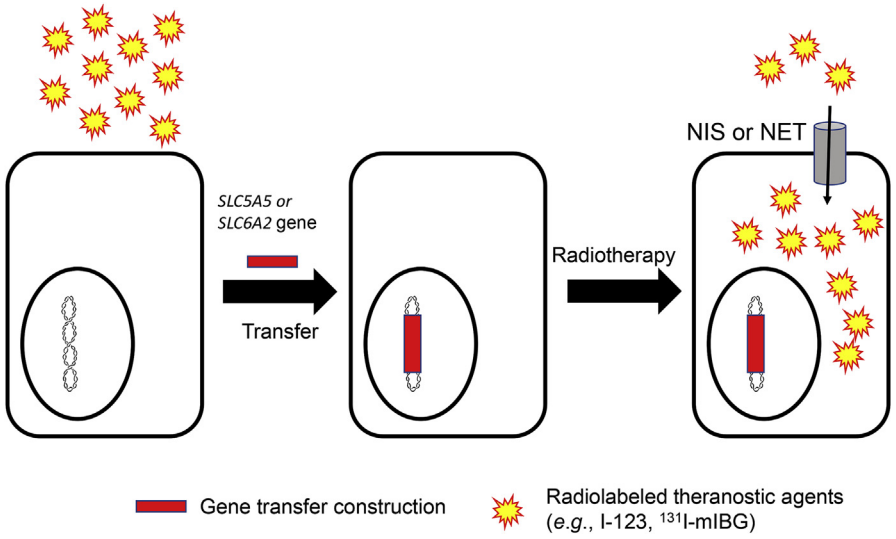

Figure 2 Strategy for targeting cancer cells transferred with NIS or NET transporters for imaging and therapy. Virus or non-virus vectors with transporter genes (NIS or NET) are constructed and transfected into cancer cells. After integrated into the host DNA, transporters can be expressed and facilitate the uptake of a theranostic agent.

resolution and tumor detection, and is now used as the gold standard for the diagnosis and monitoring therapeutic response in neuroblastoma[50]. When labeled with the β-emitter I-131, ^{131}I-mIBG becomes a powerful targeted radiopharmaceutical that can be used in the treatment of neuroblastoma and other neuroendocrine tumors (*e.g.*, pheochromocytomas).

3.2. *Molecular and physiological characteristics of NET*

NET, encoded by *SLC6A2*, belongs to the neurotransmitter transporter family[51]. It is mainly expressed at the central noradrenergic and peripheral sympathetic synapses. NET has 617 amino acids with an apparent molecular weight at around 70 kDa. The electrochemical gradient of Na^+ along the cell membrane is the energy source for the accumulation of NET substrates into the cells. Besides Na^+, Cl^- is the other critical ion needed for the normal binding of substrates to NET. The reversal of transport function can only be detected when the intracellular concentration of the substrate is high enough[51].

Since NE is the main neurotransmitter released from postganglionic sympathetic neurons, the expression and function of NET plays a crucial role in the maintenance of NE concentration in the synapse. Approximately 80%–90% of NE was taken up by NET. Besides NE, NET can also facilitate the uptake of other neurotransmitters and structurally related compounds such as dopamine, serotonin, and the neurotoxin 1-methyl-4-phenylpyridinium (MPP^+). The impaired function of NET could lead to various diseases. For example, patients with postural tachycardia syndrome are suffered from a NET-A457P mutation which could lead to an increased free NE concentration and chronically increased the heart rate[52].

3.3. *Expression of NET in neuroendocrine cancers*

In cancer, NET expression is detected in tumors derived either from neural crest in early development or from chromaffin cells of adrenal medulla[48]. The two well-studied cancers with NET expression are neuroblastoma and pheochromocytoma (PHEO). In neuroblastoma, NET mRNA expression can be detected in majority of patients whereas high protein expression has been reported in a small cohort of intermediate-to high-risk patients[47]. Meanwhile, the high NET protein expression in this cohort of patients and is also correlated with non-amplification of the oncogene *MYCN*, which is a marker for poor disease prognosis. However, expression NET protein expression was determined through subjective reading of immunohistochemistry (IHC) slides, which may not represent the protein expression of the whole tumors[53]. For PHEO, the NET mRNA expression is correlated with the genotype of tumor, and the PHEO derived by mutation at the proto-oncogene REarranged during Transfection (*RET*) has a higher mRNA expression than PHEO induced by von Hippel-Lindau (vHL) disease[54].

Because of the relatively specific expression of NET, imaging and therapeutic tools to target NET for neuroblastoma and PHEO were developed. Among them, mIBG is the most well studied compound[55], which has already been approved by FDA for imaging use for both cancers, and monotherapeutic use for PHEO.

3.4. *mIBG and other imaging agents*

mIBG was first developed to target NET in adrenal medulla as a scintigraphic tool in 1980s[49]. Among all other compounds developed and its own isomer, mIBG was more metabolically stable, and less susceptible to deiodination. Although the mechanism was not well-understood in 1984, scientists have already observed the accumulation of mIBG in the neuroblastoma[56]. Since then, numerous studies have been performed to characterize the mIBG accumulation in neuroblastoma cells, and these studies have established NET as the principal transporter responsible for cellular uptake of mIBG into neuroblastoma cells[48,50]. Currently, gamma scan with ^{123}I-mIBG is the test of choice for the detection of primary tumors and the identification of metastatic sties for neuroblastoma. It can reach 88%–93% of sensitivity and 83%–92% of specificity for neuroblastoma diagnosis[55].

As a therapeutic agent, ^{131}I-mIBG has the advantage of systemic delivery to multiple tumor sites with selective tumor targeting and killing. Historically, ^{131}I-mIBG therapy was reserved for the

treatment of neuroblastoma patients with relapsed or refractory disease[50]. Recently, several pilot studies have suggested the benefits of high dose ^{131}I-mIBG therapy when given at the time of diagnosis for high risk neuroblastoma with overall response rates ranging 30%−40%[50,57]. The major toxicity associated with high dose (>12 mCi/kg) ^{131}I-mIBG therapy is hematopoietic toxicity, which can be rescued by autologous stem cell infusion[50]. Based on these encouraging results, ^{131}I-mIBG therapy is being investigated as a frontline treatment for high risk neuroblastoma[44,50,58].

Similar to the development of radioiodine to thyroid cancer, other radioisotope labels targeting NET in neuroblastoma have also been evaluated or currently under investigation[59]. For diagnosis, ^{18}F-fluoropropylbenzylguanidine (MFBG) was tested because of F-18's potential higher sensitivity and shorter half-life[60]. A clinical study in a single patient showed similar biodistribution compare to the ^{123}I-mIBG[61], but more patients' data is needed to draw a conclusion for the further application of the MFBG. Along the same thoughts, ^{18}F-metafluorobenzylguanidine was also developed and showed promising results. Just 1 h after injection, this tracer showed a high contrast of lesion to background compare to ^{123}I- mIBG injection[62]. Other imaging tools, including ^{11}C-metahydroxyephedrine (HED)[63], ^{18}F-fluorodopamine (^{18}F-FDA)[64] and 6-^{18}F-fluoro-L-dihydroxyphenylalanine (^{18}F-DOPA)[65] are all currently under *in vitro* and *in vivo* investigations.

3.5. *Improving mIBG therapy in cancer*

In a recent study by the Children's Oncology Group[47], the correlation between NET protein and mIBG avidity has been established, suggesting that theranostic effect of mIBG can be strongly modulated by the protein expression of NET. In this study, the high-risk group neuroblastoma patients with a relatively lower expression of NET mRNA and protein, showed a negative mIBG scan result. This is potentially due to the undifferentiated state of high-risk neuroblastomas, since the NET protein expression is commonly considered as a sign of mature neuroendocrine/neural cells[48]. To improve the efficacy of mIBG scan and treatment, multiple methods have been developed to upregulate the expression of NET in high-risk neuroblastoma patients, including pretreatment of cisplatin and doxorubicin to increase NET expression[66], stimulation of differentiation of neuroblastoma by RA[67], inactivation of protein kinase C pathway[68] and more. Among these methods, the pretreatment of cisplatin and doxorubicin has shown significant increase of NET expression in clinical study and a better response to mIBG scan. The use of histone deacetylase inhibitors, such as vorinostat, can also lead to an additive effect in patients by both increasing NET expression and sensitizing cells to radiation by inhibiting the repair mechanism of DNA[69].

The major challenge and study focus of mIBG currently is the application and improvement of ^{131}I-mIBG as a theranostic tool. Currently, over 1000 patients worldwide have been treated with ^{131}I mIBG therapy. The major application of ^{131}I mIBG in the therapeutic is to be a part of the induction therapy in patients with newly diagnosed mIBG-avid neuroblastoma. Besides that, several mIBG therapeutic trails are currently on-going. These therapies cover a wide range of strategies, including mIBG monotherapy, tandem mIBG infusions, mIBG in conjunction with bone marrow transplantation and the coadministration of mIBG with radiosensitizers[55]. Though the single-agent therapy has not been approved for neuroblastoma, the application of this strategy was approved by FDA for PHOE.

Besides NET, mIBG may also be a substrate for a group of low affinity and high capacity transporters known as uptake 2, including organic cation transporters 1, 2 and 3 (OCT1−3)[70,71]. The OCTs are widely expressed in a number of normal tissues including liver, kidney, heart and salivary glands[71−73]. Coincidentally, many of these OCT-expressing tissues accumulate mIBG as revealed by ^{123}I-mIBG scintigraphy[44]. This interaction between mIBG and OCTs could lead to lower resolution for imaging and potential toxicity for the therapeutic use of mIBG. Additionally, the interaction between mIBG and the renal OCT2 could also lead to potential DDIs in kidney due to the polypharmacy during chemotherapy[72]. The inhibition of OCTs may help reducing mIBG accumulation and toxicity in normal tissues.

4. GLUT1 and ^{18}F-FDG tumor imaging

4.1. *Clinical background*

In the 1920s, Warburg and colleagues[74] made the observation that tumors were taking up enormously more amounts of glucose than the surrounding normal tissue. Further, unlike normal cells, which produce energy from oxidative phosphorylation of glucose, most cancer cells predominantly produce energy through aerobic glycolysis of glucose to produce lactate. This phenomenon, known as the Warburg Effect, forms the basis for the development of the radioactive glucose analog ^{18}F fluorodeoxyglucose (^{18}F-FDG) as a cancer imaging agent (Fig. 1). Combined with PET/CT scanning, ^{18}F-FDG PET can non-invasively determine the location and metabolism of tumors, and help quantitatively staging of tumors[75]. Currently, ^{18}F-FDG PET is widely applied in the diagnosis, staging and therapy progress monitoring of different cancers, including non-small cell lung cancer, lymphoma, ovarian cancer, kidney cancer, etc[76]. Glucose transporter 1 (GLUT1), a hypoxia-responsive transporter, is believed to play a predominant role in mediating tumor uptake of ^{18}F-FDG (Fig. 3)[77].

4.2. *Molecular and physiological characteristics of GLUTs*

GLUT1 belongs to *SLC2* family, encoded by *SLC2A1*, which is one of the first identified transporter[78]. Till now, 14 members of *SLC2* family have been characterized. GLUTs are probably the most well-studied human transporters because of their early discovery as well as important roles in glucose uptake[79]. GLUT1 functions as a facilitative uniporter. The major physiological substrate of GLUT1 is glucose (K_m = 3 mmol/L), but it can also transport mannose, galactose, glucosamine and some other hexoses. GLUT1 expression occurs in almost all tissues, with high expression typically found in tissues with high cellular glucose metabolism. In normal tissues, the highest expression of GLUT1 can be found erythrocytes and endothelial cells forming blood−brain barrier[80], which respectively increases the glucose carrying capacity in red blood cells and supports glucose supply to the brain[79,80].

4.3. *Expression of GLUT1 in cancers and correlation with clinical prognosis*

Overexpression of GLUTs, especially GLUT1, has been frequently observed in numerous human carcinomas. Upregulation of GLUT1 expression has been observed in a broad spectrum of tumors, including pancreatic cancer, breast cancer, lymphomas,

prostate cancer, head, neck cancer, etc[81,82]. However, GLUT1 expression has been reported to be absent in certain cancers (*e.g.*, sarcomas and melanomas), suggesting that other GLUTs may mediate the glycolytic pathway in these tumors[82]. Many studies have reported a correlation between GLUT1 expression level and the grade of tumor aggressiveness, which suggests that GLUT1 expression may be of prognostic significance. For example, a recent meta-analysis study summarized 26 clinical studies with 2948 patients across several different tumors using GLUT1 as a prognosis marker, and the meta-analysis suggested that the GLUT1 high expression is positively correlated with overall unfavorable clinical outcome (3- and 5-year overall survival (OS) and 5-year disease-free survival)[83]. A detailed analysis also showed adverse OS is correlated with GLUT1 expression in oral squamous cell carcinoma and breast cancer, but not with colorectal cancer, lung cancer, cervical cancer and pancreatic cancer[83].

4.4. *^{18}F-FDG and its clinical application*

Because of the high glucose uptake rate in malignant tumors, ^{18}F-FDG was developed to be used as an imaging and staging agent for cancer. Combined with PET/CT scanning, ^{18}F-PET can non-invasively determine the metabolism of tumors, and help quantitatively staging of tumors[75]. The mechanism of ^{18}F-FDG PET is based on the fact that the higher glucose uptake usually reflects larger tumor sizes or worse malignancy, so that the higher FDG signals around lesion the more advanced stage of tumor. ^{18}F-FDG was first approved in 2000 by FDA for assisting the evaluation of malignancy in patients with known or suspected abnormalities found by other testing modalities, or in patients with an existing diagnosis of cancer[84].

Currently, ^{18}F-FDG PET is widely applied in the staging and therapeutic progress monitoring of different cancers. The International Atomic Energy Agency (IAEA) defined that the "appropriate use" of ^{18}F-FDG PET in patients should meet the conditions including evidences of improved diagnostic performance comparing to other current techniques, results that can influence clinical practice and plausible impact on the patient's outcome[85]. Even under such a high standard, IAEA recommended that ^{18}F-FDG PET can be appropriately used in the diagnosis, staging, response evaluation, restaging, suspected recurrence, follow-up and radiotherapy preparing of 21 different cancers, including non-small cell lung cancer, lymphoma, ovarian cancer, kidney cancer, etc[76]. However, the relative high false-positive rate and low efficacy in certain cancers was the main challenge for this modality[86]. Although CT has been combined with ^{18}F-FDG PET scanning to improve the technique, ^{18}F-FDG PET is still mainly applied as the additional modality to confirm the finding of a new lesion and stage the existing lesion[87].

4.5. *Correlation between GLUT1 expression and ^{18}F-FDG uptake*

As the major uptake transporter of ^{18}F-FDG in tumors, the expression and function of GLUT1 and other *SLC2* family members is crucial for the efficacy of ^{18}F-FDG PET. Many studies have been conducted to illustrate the relationship between GLUT1 expression and ^{18}F-FDG PET efficacy. However, the results are not consistent in different cancers. In salivary gland pleomorphic adenomas, the higher GLUT1 protein expression is correlated with a better standardized uptake value (SUV) for ^{18}F-FDG[88]. In hepatocellular carcinoma, the ^{18}F-FDG SUV can also be correlated with GLUT1, pSTAT3 and HIF1α expression rather than other *SLC2* family members (GLUT2, GLUT3 and GLUT4), and the GLUT1 expression is also a marker for poor differentiation and vascular invasion[89]. The GLUT1 expression in hepatocellular carcinoma is also correlated with the proliferative activity, suggesting highly GLUT expression is correlated with poor disease prognosis[90]. Similar observations can be seen in pancreatic cancer[91], thymic epithelial tumors[92] and other fast growing cancers[93]. However, some tumors, such as colorectal adenocarcinoma[94] and pancreatobiliary cancer, the GLUT1 expression appears not correlated with ^{18}F-FDG SUV, suggesting that other GLUTs (*e.g.*, GLUT3) may be involved.

As GLUT1 expression is correlated with both ^{18}F-FDG SUV and clinical outcome in several cancers, studies have also been done to demonstrate that the high ^{18}F-FDG PET imaging response can be used as a poor prognostic factor in certain cancers. For example, the high ^{18}F-FDG SUV in breast cancer has been proved to be associated with poor prognosis in a clinical study with 131 patients[95].

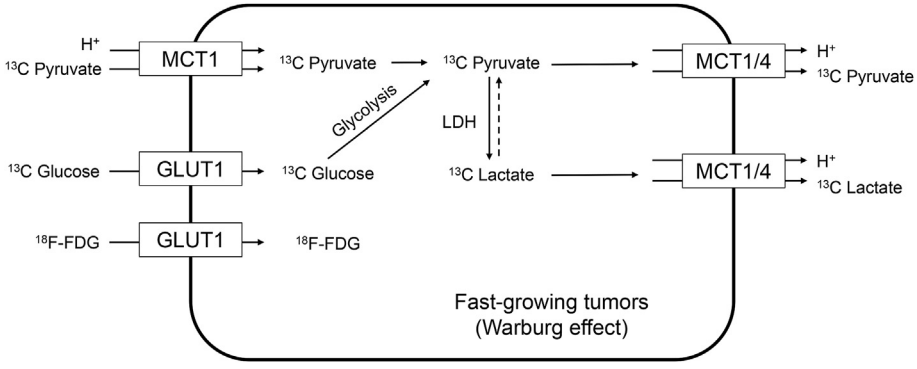

Figure 3 Targeting GLUT1, MCT1 and MCT4 for cancer imaging or metabolic imaging. MCT1 and GLUT1 can transport hyperpolarized ^{13}C labeled agents into the fast-growing tumor cells. Hyperpolarized MRI scanning can capture signals of both the uptake of labeled parent agents and their metabolites, and the metabolic rate can be estimated. The signals for further efflux or metabolites can also be used for the analysis of invasiveness of disease. ^{18}F-FDG can be transported into fast-growing tumors with a higher rate compared to normal tissue due to the Warburg effect.

4.6. *Improving GLUT-mediated cancer imaging*

One of the major shortcomings of ^{18}F-FDG PET is that when used as a diagnostic tool, the sensitivity and specificity is limited due to the low expression of GLUT1 in some cancers, which could lead to lower efficacy[96]. One approach to improve this limitation is to target other members of GLUT family which are also expressed in tumors. In breast cancer, GLUT5 protein expression can also be detected[97], and 6-^{18}F-fluoro-D-fructose (6-^{18}F-FDF) and several other analogs were developed to target GLUT5 in breast cancer cell lines and xenograft mouse[98]. Though the mouse 6-^{18}F-FDF PET imaging signals were still not comparable to ^{18}F-FDG PET signals, this approach could be an alternative way to target GLUTs for cancer imaging in the future.

5. MCT1/4 and hyperpolarized ^{13}C MRI

5.1. *Clinical background*

As fast-growing tissues, tumors require high energy intake and are often present in an anaerobic microenvironment, which makes the expression and function of transporters and enzymes involved in glycolysis crucial for tumor growing. For hypoxia tumor cells, glycolysis is used to generate energy with lactate being produced due to the lack of oxygen. Even for oxygenated cells, Warburg effect occurs and glycolysis, rather than oxidative phosphorylation, is the main pathway of energy production[99], which also leads to the byproduct of lactate and pyruvate. Monocarboxylate transporters (MCTs), which transport short chain monocarboxylate including L-lactate and pyruvate, have important functions in the maintenance of cellular metabolism in tumor cells[100,101]. MCTs, such as MCT1 and MCT4, are currently being investigated as potential drug target for cancer treatment, especially in cancers with a hyper-glycolytic and acid-resistant phenotype[102].

Besides being a therapeutic target, MCTs are also a diagnostic and monitoring target by using hyperpolarized ^{13}C MRI technique. Hyperpolarized ^{13}C MRI is a recent developed technique to not only detect the path or accumulation of labelled probes, but also the cell metabolism of the probes[103]. Recent development in cancer cell metabolism generated more detailed picture of the metabolite pathway for probes like pyruvate and lactate, which enlightened the use of ^{13}C-pyruvate and ^{13}C-lactate (Fig. 1) as a diagnostic agent and treatment progress monitor for cancers with high glycolysis profile. In this case, the expression and function of MCTs is crucial for the proper application of this technique.

5.2. *Molecular and physiological characteristics of MCTs*

MCTs belong to *SLC16* family and were first identified in the mid-nineties[104]. Among 14 members of this gene family, four genes (*SLC16A1*, *SLC16A3*, *SLC16A7* and *SLC16A8*) encode the proton-coupled monocarboxylate transporters, namely MCT1, MCT4, MCT2 and MCT3[105]. MCT1−MCT4 are proton-coupled symporters and their main function is to facilitate the transport of a broad spectrum of short chain monocarboxylates (*e.g.*, lactate, pyruvate, and ketone bodies) across the membrane[106]. Although both endo- and exogenous inhibitors have been identified for MCTs, such as stilbene disulphonates and quercetins[107], no MCT specific inhibitors has been developed.

Among the MCTs, MCT1 and MCT4 are most well-studied members. The two transporters share similar endogenous substrates, but play separate physiological roles because of their different affinity to lactate and pyruvate[105]. MCT1 has a relatively higher affinity for lactate (K_m = 4.5 mmol/L) and pyruvate (K_m = 0.7 mmol/L) than MCT4 (K_m = 28 and 153 mmol/L, respectively)[108,109]. This affinity combination explains the function of these two transporters: for glycolytic cells, MCT1 is responsible for the efflux of lactate while MCT4 is expressed to build up the internal concentration of pyruvate; for other cells require lactate for lipogenesis and gluconeogenesis, MCT1 is usually expressed to facilitate the uptake of lactate[105].

Because of their crucial roles in glycolysis, MCT1 and MCT4 are widely expressed across human body and are involved in different metabolism of nutrients. MCT1 is ubiquitously expressed except β cells in pancreases[105], and MCT4 can be detected in skeletal muscle, chondrocytes, leucocytes, testis, lung, ovary, placenta and heart[110]. The silence or overexpression of MCT1 and MCT4 appear to be associated with several pathological conditions, including hyperinsulinism[111], inflammatory bowel disease[112] and fatigue syndromes[113].

5.3. *Expression and function of MCT1 and MCT4 in cancer*

MCT1 and MCT4 expression have been reported to be expressed in many different kinds of tumors, including head and neck, breast, lung, bladder, prostate, glioma, etc.[100,102,114,115], although conflicting results also exist[101]. As most solid tumors rely on glycolysis for energy production, a large amount of lactate are produced and exported into the extracellular milieu, contributing to the acidic microenvironment. MCTs have been proposed to play a dual role in the maintenance of the hyper-glycolytic acid-resistant phenotype of cancer cells by mediating lactate efflux and pH regulation through the co-transport of protons[101]. Functioning as bi-directional transporters, MCTs can also mediate cellular uptake of imaging and/or therapeutic agents in cancer cells (Fig. 3). As their expression is elevated in cancer cells, MCTs can be targeted to selectively image cancer cells and/or deliver therapeutic agents into cancer cells.

5.4. *MCT1 and MCT4 in hyperpolarized ^{13}C MRI*

Currently, the application of hyperpolarized ^{13}C MRI technique is still under development and limited to a small portion of patients because of the complexity, expense and requirement for administrating an imaging agent[103]. Several clinical trials are ongoing to investigate the use of hyperpolarized ^{13}C MRI with ^{13}C-pyruvate and ^{13}C-lactate as a diagnostic tool for different cancers including locally advanced cervical cancer (LACC), prostate cancer, central nervous system cancer, etc. The aims of the majority of the clinical studies are focused on the evaluation of the efficiency of hyperpolarized ^{13}C MRI as a diagnostic tool[103]. The contribution of MCT1 and MCT4 in pyruvate or lactate-based hyperpolarized ^{13}C MRI is still largely unknown. Nevertheless, MCT1 and MCT4 are the major transporters for lactate and pyruvate in cancers, and many studies have investigated the mechanisms and consequences of MCT1 and MCT4 expression in cancers. It has been reported that when MCT1 was inhibited or knocked down, both cancer cell lines and xenografted mouse with human lung carcinoma or colorectal adenocarcinoma cells lost the function of utilizing lactate as an energy source[114]. It was also demonstrated that when *MCT1* gene was knocked out, the migration and invasion ability of cancer cells reduced significantly due to impaired lactate efflux and extracellular acidification[116,117]. Clinico-pathological study of MCT1 in

endometrial cancer also suggested that the high MCT1 expression is a marker for poor prognosis[118]. Based on these studies, it is suggested that the flux rate of lactate in some cancers is determined by the expression of MCT1, and the flux rate of lactate can be a biomarker for malignancy of these cancers. In one on-going clinical study (NCT03129776), hyperpolarized ^{13}C-lactate is injected to patients with LACC and imaged with MRI. The results will be compared with ^{18}F-FDG PET, and additional and more specific information regarding the metabolic activity are expected.

^{13}C-pyruvate is also being investigated as a diagnostic tool for several different cancers, besides its ability to be accumulated in tumors, the metabolism rate of pyruvate into lactate is also a sign for the malignancy. *In vitro* and *in vivo* studies with hyperpolarized ^{13}C-pyruvate have shown that in renal cell carcinoma, after being transported into the cancer cells through MCT1, with the help of LDH, ^{13}C-pyruvate can be converted into ^{13}C-lactate, and then further exported out of the cells through MCT4[119,120]. This process generates a unique pattern in patients with malignant tumors by MRI, which showed not only a pyruvate peak, but also a lactate peak[121,122]. While still under development, the feasibility of hyperpolarized ^{13}C-pyruvate MRI to inform on tumor lactate production and dynamics provides scientific premise for future clinical investigation into the utility of this technique to noninvasively assess tumor aggressiveness and guide treatment selection.

6. Summary and perspectives

In this review, we focus on several SLC transporters known to be involved in targeting clinically used imaging and theranostic agents for cancer diagnosis and treatment (Table 1). It is our hope that these clinically successful cases would serve examples to foster interest in basic and translational research in membrane transporters and their potential applications in cancer diagnosis and treatment. Besides the transporters discussed above, several other SLC transporters are being used or investigated for targeting imaging agents or drugs in cancer. For example, ^{11}C-methionine is an amino acid tracer used in PET imaging of brain tumors, and its tumor uptake is likely mediated by the large amino acid transporter 1 (LAT1)[123,124].

As illustrated in the above examples, several key features are essential for successful targeting imaging and therapeutic agent into cancer cells. First, the targeted transporters should be highly, preferably specifically, expressed in tumor cells to ensure high uptake in tumor as compared to normal tissues. Second, the imaging agent should be specific for the targeted transporter to ensure a high tumor-to-background ratio. This could be challenging as many SLC transporters have gene homologs with large overlap in substrate specificity. Third, the chemical structure of the imaging agent should contain an element amenable for radioisotope labeling and compatible with imaging modalities. Lastly, as the imaging agent will eventually be administrated to humans, it should also possess suitable pharmacokinetic properties and reasonable safety margins.

Cancer patients often take multiple drugs to treat comorbidities, control pains, or relieve severe side effects (*e.g.*, nausea) associated with chemo- or radiation therapy. Inhibition of transporters responsible for tumor uptake of an imaging or therapeutic agent could lead to misdiagnosis and therapeutic failures. Clinical application of transporter-mediated tumor targeting must consider potential interactions between the radiopharmaceuticals and concurrently used medications. For example, NET is a major target of tricyclic antidepressants (TCAs) and serotonin-norepinephrine reuptake inhibitors (SNRIs), which exhibit their pharmacological effects in part by blocking NET-mediated presynaptic reuptake of NE. Use of such drugs should be avoided before and during mIBG imaging and therapy. In addition, like other small molecule drugs, radiopharmaceuticals are eliminated from the systemic circulation mainly by the liver and/or kidney. Inhibition or induction of drug-metabolizing enzymes and transporters involved in their hepatic or renal elimination could lead to adverse DDIs due to altered systemic exposure to the radiopharmaceuticals. Unfortunately, drug interactions with radiopharmaceuticals have not been adequately studied either at the mechanistic levels or in clinical settings. This would represent an important area for future research.

The SLC superfamily consists of more than 400 membrane transport proteins with diverse function and tissue distribution. While a large portion of its individual members are still poorly understood, substantial progress has been made in the past two decades in the identification and characterization of many novel SLC members. Further understanding of the structure, function, expression and regulation of SLC transporters in cancer could lead to many opportunities to explore novel targets and agents for cancer imaging and treatment. With the advancement in new imaging technology and modalities, molecularly targeting uptake transporters uniquely enriched in tumor cells holds great promise for the development of new imaging applications that can give crucial information about not only the localization of the tumor, but also tumor progression, aggressiveness, and response to therapy in clinical setting. Understanding the impact and mechanisms of drug interactions with transporter-targeted radiopharmaceuticals can further improve their clinical use and applications. Advancement in these research areas is expected to benefit cancer patients by facilitating cancer diagnosis, staging, radiotherapy as well as guiding treatment plans for individual patients.

Acknowledgment

This study was supported by the National Institutes of Health (NIH) National Institute of General Medical Sciences (Grant R01 GM066233, USA). The content is solely the responsibility of the authors and does not necessarily represent the official views of the NIH.

Author contributions

Yuchen Zhang was responsible for investigation, data curation, visualization, and original draft preparation. Joanne Wang was responsible for conceptualization, methodology, original draft preparation, reviewing and editing, and funding acquisition.

Conflicts of interest

The authors declare no conflicts of interest.

References

1. Schiffman JD, Fisher PG, Gibbs P. Early detection of cancer: past, present, and future. *Am Soc Clin Oncol Educ Book* 2015;**35**:57–65.
2. Frangioni JV. New technologies for human cancer imaging. *J Clin Oncol* 2008;**26**:4012–21.
3. Fass L. Imaging and cancer: a review. *Mol Oncol* 2008;**2**:115–52.

4. Gambhir SS. Molecular imaging of cancer with positron emission tomography. *Nat Rev Cancer* 2002;**2**:683−93.
5. Del Monte U. Does the cell number 10^9 still really fit one gram of tumor tissue?. *Cell Cycle* 2009;**8**:505−6.
6. Weissleder R. Molecular imaging in cancer. *Science* 2006;**312**: 1168−71.
7. Lin L, Yee SW, Kim RB, Giacomini KM. SLC transporters as therapeutic targets: emerging opportunities. *Nat Rev Drug Discov* 2015;**14**:543−60.
8. International Transporter Consortium, Giacomini KM, Huang SM, Tweedie DJ, Benet LZ, Brouwer K, et al. Membrane transporters in drug development. *Nat Rev Drug Discov* 2010;**9**:215−36.
9. FDA. *In vitro metabolism and transporter-mediated drug−drug interaction studies: guidance for industry.* 2017. Available from: https://www.fda.gov/downloads/Drugs/Guidances/UCM581965.pdf.
10. Mao Q, Lai Y, Wang J. Drug transporters in xenobiotic disposition and pharmacokinetic prediction. *Drug Metab Dispos* 2018;**46**: 561−6.
11. Kogai T, Brent GA. The sodium iodide symporter (NIS): regulation and approaches to targeting for cancer therapeutics. *Pharmacol Ther* 2012;**135**:355−70.
12. Verburg FA, Brans B, Mottaghy FM. Molecular nuclear therapies for thyroid carcinoma. *Methods* 2011;**55**:230−7.
13. Dai G, Levy O, Carrasco N. Cloning and characterization of the thyroid iodide transporter. *Nature* 1996;**379**:458−60.
14. Smanik A, Ryu KY, Theil KS, Mazzaferri EL, Jhiang SM. Expression, exon-intron organization, and chromosome mapping of the human sodium iodide symporter. *Endocrinology* 1997;**138**:3555−8.
15. Dohán O, De la Vieja A, Paroder V, Riedel C, Artani M, Reed M, et al. The sodium/iodide symporter (NIS): characterization, regulation, and medical significance. *Endocr Rev* 2003;**24**:48−77.
16. Dohan O, Portulano C, Basquin C, Reyna-Neyra A, Amzel LM, Carrasco N. The Na^+/I symporter (NIS) mediates electroneutral active transport of the environmental pollutant perchlorate. *Proc Natl Acad Sci U S A* 2007;**104**:20250−5.
17. Kogai T, Endo T, Saito T, Miyazaki A, Kawaguchi A, Onaya T. Regulation by thyroid-stimulating hormone of sodium/iodide symporter gene expression and protein levels in FRTL-5 cells. *Endocrinology* 1997;**138**:2227−32.
18. Jhiang SM, Cho JY, Ryu KY, DeYoung BR, Smanik A, McGaughy VR, et al. An immunohistochemical study of Na^+/I^- symporter in human thyroid tissues and salivary gland tissues. *Endocrinology* 1998;**139**:4416−9.
19. Tazebay UH, Wapnir IL, Levy O, Dohan O, Zuckier LS, Zhao QH, et al. The mammary gland iodide transporter is expressed during lactation and in breast cancer. *Nat Med* 2000;**6**:871−8.
20. Ravera S, Reyna-Neyra A, Ferrandino G, Amzel LM, Carrasco N. The sodium/iodide symporter (NIS): molecular physiology and preclinical and clinical applications. *Annu Rev Physiol* 2017;**79**:261−89.
21. Kogai T. Sodium iodide symporter in the fight against thyroid cancer. *Future Oncol* 2013;**9**:1679−82.
22. Ahn BC. Sodium iodide symporter for nuclear molecular imaging and gene therapy: from bedside to bench and back. *Theranostics* 2012;**2**:392−402.
23. Gaitan-Hernandez R. Characterization and fruit-body production of neolentinus suffrutescens strains obtained by crossing *in vitro* in a pilot plant. *Rev Iberoam Micol* 2000;**17**:20−4.
24. Wong KK, Zarzhevsky N, Cahill JM, Frey KA, Avram AM. Hybrid SPECT-CT and PET-CT imaging of differentiated thyroid carcinoma. *Br J Radiol* 2009;**82**:860−76.
25. Singh N, Lewington V. Molecular radiotheragnostics in thyroid disease. *Clin Med (Lond)* 2017;**17**:453−7.
26. Lee WW, Moon DH, Park SY, Jin J, Kim SJ, Lee H. Imaging of adenovirus-mediated expression of human sodium iodide symporter gene by ^{99m}TcO4 scintigraphy in mice. *Nucl Med Biol* 2004;**31**:31−40.
27. Chen L, Altman A, Mier W, Lu H, Zhu R, Haberkorn U. ^{99m}Tc-pertechnetate uptake in hepatoma cells due to tissue-specific human sodium iodide symporter gene expression. *Nucl Med Biol* 2006;**33**: 575−80.
28. Schipper ML, Riese CG, Seitz S, Weber A, Behe M, Schurrat T, et al. Efficacy of ^{99m}Tc pertechnetate and ^{131}I radioisotope therapy in sodium/iodide symporter (NIS)-expressing neuroendocrine tumors *in vivo*. *Eur J Nucl Med Mol Imaging* 2007;**34**:638−50.
29. Zuckier LS, Dohan O, Li Y, Chang CJ, Carrasco N, Dadachova E. Kinetics of perrhenate uptake and comparative biodistribution of perrhenate, pertechnetate, and iodide by NaI symporter-expressing tissues *in vivo*. *J Nucl Med* 2004;**45**:500−7.
30. Van Sande J, Massart C, Beauwens R, Schoutens A, Costagliola S, Dumont JE, et al. Anion selectivity by the sodium iodide symporter. *Endocrinology* 2003;**144**:247−52.
31. Jauregui-Osoro M, Sunassee K, Weeks AJ, Berry DJ, Paul RL, Cleij M, et al. Synthesis and biological evaluation of [^{18}F]tetrafluoroborate: a PET imaging agent for thyroid disease and reporter gene imaging of the sodium/iodide symporter. *Eur J Nucl Med Mol Imaging* 2010;**37**:2108−16.
32. Min JJ, Chung JK, Lee YJ, Jeong JM, Lee DS, Jang JJ, et al. Relationship between expression of the sodium/iodide symporter and ^{131}I uptake in recurrent lesions of differentiated thyroid carcinoma. *Eur J Nucl Med* 2001;**28**:639−45.
33. Chung JK, Youn HW, Kang JH, Lee HY, Kang KW. Sodium iodide symporter and the radioiodine treatment of thyroid carcinoma. *Nucl Med Mol Imaging* 2010;**44**:4−14.
34. Ward LS, Santarosa L, Granja F, da Assumpcao LV, Savoldi M, Goldman GH. Low expression of sodium iodide symporter identifies aggressive thyroid tumors. *Cancer Lett* 2003;**200**:85−91.
35. Kogai T, Curcio F, Hyman S, Cornford EM, Brent GA, Hershman JM. Induction of follicle formation in long-term cultured normal human thyroid cells treated with thyrotropin stimulates iodide uptake but not sodium/iodide symporter messenger RNA and protein expression. *J Endocrinol* 2000;**167**:125−35.
36. Riedel C, Levy O, Carrasco N. Post-transcriptional regulation of the sodium/iodide symporter by thyrotropin. *J Biol Chem* 2001;**276**: 21458−63.
37. Ladenson W, Braverman LE, Mazzaferri EL, Brucker-Davis F, Cooper DS, Garber JR, et al. Comparison of administration of recombinant human thyrotropin with withdrawal of thyroid hormone for radioactive iodine scanning in patients with thyroid carcinoma. *N Engl J Med* 1997;**337**:888−96.
38. Kogai T, Schultz JJ, Johnson LS, Huang M, Brent GA. Retinoic acid induces sodium/iodide symporter gene expression and radioiodide uptake in the MCF-7 breast cancer cell line. *Proc Natl Acad Sci U S A* 2000;**97**:8519−24.
39. Schmutzler C, Winzer R, Meissner-Weigl J, Kohrle J. Retinoic acid increases sodium/iodide symporter mRNA levels in human thyroid cancer cell lines and suppresses expression of functional symporter in nontransformed FRTL-5 rat thyroid cells. *Biochem Biophys Res Commun* 1997;**240**:832−8.
40. Hingorani M, Spitzweg C, Vassaux G, Newbold K, Melcher A, Pandha H, et al. The biology of the sodium iodide symporter and its potential for targeted gene delivery. *Curr Cancer Drug Targets* 2010;**10**:242−67.
41. Dwyer RM, Bergert ER, O'Connor MK, Gendler SJ, Morris JC. Adenovirus-mediated and targeted expression of the sodium-iodide symporter permits *in vivo* radioiodide imaging and therapy of pancreatic tumors. *Hum Gene Ther* 2006;**17**:661−8.
42. Brodeur GM. Neuroblastoma: biological insights into a clinical enigma. *Nat Rev Cancer* 2003;**3**:203−16.
43. Brodeur GM, Iyer R, Croucher JL, Zhuang T, Higashi M, Kolla V. Therapeutic targets for neuroblastomas. *Expert Opin Ther Targets* 2014;**18**:277−92.
44. Park JR, Bagatell R, London WB, Maris JM, Cohn SL, Mattay KK, et al. Children's oncology group's 2013 blueprint for research: neuroblastoma. *Pediatr Blood Cancer* 2013;**60**:985−93.
45. Park JR, Eggert A, Caron H. Neuroblastoma: biology, prognosis, and treatment. *Hematol Oncol Clin N Am* 2010;**24**:65−86.

46. Carlin S, Mairs RJ, McCluskey AG, Tweddle DA, Sprigg A, Estlin C, et al. Development of a real-time polymerase chain reaction assay for prediction of the uptake of meta-[^{131}I]iodobenzylguanidine by neuroblastoma tumors. *Clin Cancer Res* 2003;**9**:3338−44.
47. Dubois SG, Geier E, Batra V, Yee SW, Neuhaus J, Segal M, et al. Evaluation of norepinephrine transporter expression and meta-iodobenzylguanidine avidity in neuroblastoma: a report from the children's oncology group. *Int J Mol Imaging* 2012;**2012**:250834.
48. Streby KA, Shah N, Ranalli MA, Kunkler A, Cripe T. Nothing but NET: a review of norepinephrine transporter expression and efficacy of ^{131}I-mIBG therapy. *Pediatr Blood Cancer* 2015;**62**:5−11.
49. Wieland DM, Wu J, Brown LE, Mangner TJ, Swanson D, Beierwaltes WH. Radiolabeled adrenergi neuron-blocking agents: adrenomedullary imaging with [^{131}I]iodobenzylguanidine. *J Nucl Med* 1980;**21**:349−53.
50. Parisi MT, Eslamy H, Park JR, Shulkin BJ, Yanik GA. ^{131}I-Meta-iodobenzylguanidine theranostics in neuroblastoma: historical perspectives; practical applications. *Semin Nucl Med* 2016;**46**:184−202.
51. Mandela P, Ordway GA. The norepinephrine transporter and its regulation. *J Neurochem* 2006;**97**:310−33.
52. Shirey-Rice JK, Klar R, Fentress HM, Redmon SN, Sabb TR, Krueger JJ, et al. Norepinephrine transporter variant A457P knock-in mice display key features of human postural orthostatic tachycardia syndrome. *Dis Model Mech* 2013;**6**:1001−11.
53. van Berkel A, Rao JU, Lenders JW, Pellegata NS, Kusters B, Piscaer I, et al. Semiquantitative ^{123}I-metaiodobenzylguanidine scintigraphy to distinguish pheochromocytoma and paraganglioma from physiologic adrenal uptake and its correlation with genotype-dependent expression of catecholamine transporters. *J Nucl Med* 2015;**56**:839−46.
54. Saveanu A, Muresan M, de Micco C, Taieb D, Germanetti AL, Sebag F, et al. Expression of somatostatin receptors, dopamine D_2 receptors, noradrenaline transporters, and vesicular monoamine transporters in 52 pheochromocytomas and paragangliomas. *Endocr Relat Cancer* 2011;**18**:287−300.
55. Sharp SE, Trout AT, Weiss BD, Gelfand MJ. MIBG in neuroblastoma diagnostic imaging and therapy. *RadioGraphics* 2016;**36**:258−78.
56. Treuner J, Feine U, Niethammer D, Muller-Schaumburg W, Meinke J, Eibach E, et al. Scintigraphic imaging of neuroblastoma with [^{131}-I]iodobenzylguanidine. *Lancet* 1984;**1**:333−4.
57. Wilson JS, Gains JE, Moroz V, Wheatley K, Gaze MN. A systematic review of ^{131}I-*meta* iodobenzylguanidine molecular radiotherapy for neuroblastoma. *Eur J Cancer* 2014;**50**:801−15.
58. Irwin MS, Park JR. Neuroblastoma: paradigm for precision medicine. *Pediatr Clin N Am* 2015;**62**:225−56.
59. Pandit-Taskar N, Modak S. Norepinephrine transporter as a target for imaging and therapy. *J Nucl Med* 2017;**58**:39S−53S.
60. Vaidyanathan G, Affleck DJ, Zalutsky MR. No-carrier-added (4-fluoro-3-[^{131}I]iodobenzyl)guanidine and (3-[^{211}At]astato-4-fluorobenzyl)guanidine. *Bioconjug Chem* 1996;**7**:102−7.
61. Suh M, Park HJ, Choi HS, So Y, Lee BC, Lee WW. Case report of PET/CT imaging of a patient with neuroblastoma using ^{18}F-FPBG. *Pediatrics* 2014;**134**:e1731−4.
62. Pandit-Taskar N, Zanzonico P, Staton KD, Carrasquillo JA, Reidy-Lagunes D, Lyashchenko S, et al. Biodistribution and dosimetry of ^{18}F-*meta*-fluorobenzylguanidine: a first-in-human PET/CT imaging study of patients with neuroendocrine malignancies. *J Nucl Med* 2018;**59**:147−53.
63. Bonfiglioli R, Nanni C, Martignani C, Zanoni L, La Donna R, Diemberger I, et al. ^{11}C-mHED for PET/CT: principles of synthesis, methodology and first clinical applications. *Curr Radiopharm* 2014;**7**:79−83.
64. Ding YS, Fowler JS, Gatley SJ, Dewey SL, Wolf A, Schlyer DJ. Synthesis of high specific activity 6-[^{18}F]fluorodopamine for positron emission tomography studies of sympathetic nervous tissue. *J Med Chem* 1991;**34**:861−3.
65. Minn H, Kemppainen J, Kauhanen S, Forsback S, Seppanen M. ^{18}F-fluorodihydroxyphenylalanine in the diagnosis of neuroendocrine tumors. *PET Clin* 2014;**9**:27−36.
66. Mastrangelo R, Tornesello A, Lasorella A, Iavarone A, Mastrangelo S, Riccardi R, et al. Optimal use of the ^{131}I-meta-iodobenzylguanidine and cisplatin combination in advanced neuroblastoma. *J Neuro Oncol* 1997;**31**:153−8.
67. Rutgers M, Buitenhuis CK, Hoefnagel CA, Voute A, Smets LA. Targeting of *meta*-iodobenzylguanidine to SK-N-SH human neuroblastoma xenografts: tissue distribution, metabolism and therapeutic efficacy. *Int J Cancer* 2000;**87**:412−22.
68. Apparsundaram S, Galli A, DeFelice LJ, Hartzell HC, Blakely RD. Acute regulation of norepinephrine transport: I. protein kinase C-linked muscarinic receptors influence transport capacity and transporter density in SK-N-SH cells. *J Pharmacol Exp Ther* 1998;**287**:733−43.
69. Mueller S, Yang X, Sottero TL, Gragg A, Prasad G, Polley MY, et al. Cooperation of the HDAC inhibitor vorinostat and radiation in metastatic neuroblastoma: efficacy and underlying mechanisms. *Cancer Lett* 2011;**306**:223−9.
70. Duan H, Wang J. Selective transport of monoamine neurotransmitters by human plasma membrane monoamine transporter and organic cation transporter 3. *J Pharmacol Exp Ther* 2010;**335**:743−53.
71. Wagner DJ, Hu T, Wang J. Polyspecific organic cation transporters and their impact on drug intracellular levels and pharmacodynamics. *Pharmacol Res* 2016;**111**:237−46.
72. Yin J, Wang J. Renal drug transporters and their significance in drug−drug interactions. *Acta Pharm Sin B* 2016;**6**:363−73.
73. Lee N, Duan H, Hebert MF, Liang CJ, Rice KM, Wang J. Taste of a pill: organic cation transporter-3 (OCT3) mediates metformin accumulation and secretion in salivary glands. *J Biol Chem* 2014;**289**:7055−64.
74. Liberti MV, Locasale JW. The Warburg Effect: how does it benefit cancer cells?. *Trends Biochem Sci* 2016;**41**:211−8.
75. Weber WA, Schwaiger M, Avril N. Quantitative assessment of tumor metabolism using FDG-PET imaging. *Nucl Med Biol* 2000;**27**:683−7.
76. Fletcher JW, Djulbegovic B, Soares H, Siegel BA, Lowe VJ, Lyman GH, et al. Recommendations on the use of ^{18}F-FDG PET in oncology. *J Nucl Med* 2008;**49**:480−508.
77. Ancey B, Contat C, Meylan E. Glucose transporters in cancer—from tumor cells to the tumor microenvironment. *FEBS J* 2018;**285**:2926−43.
78. Mueckler M, Caruso C, Baldwin SA, Panico M, Blench I, Morris HR, et al. Sequence and structure of a human glucose transporter. *Science* 1985;**229**:941−5.
79. Mueckler M, Thorens B. The SLC2 (GLUT) family of membrane transporters. *Mol Asp Med* 2013;**34**:121−38.
80. Dahlin A, Royall J, Hohmann JG, Wang J. Expression profiling of the solute carrier gene family in the mouse brain. *J Pharmacol Exp Ther* 2009;**329**:558−70.
81. Yamamoto T, Seino Y, Fukumoto H, Koh G, Yano H, Inagaki N, et al. Over-expression of facilitative glucose transporter genes in human cancer. *Biochem Biophys Res Commun* 1990;**170**:223−30.
82. Carvalho KC, Cunha IW, Rocha RW, Ayala FR, Cajaiba MM, Begnami MD, et al. GLUT1 expression in malignant tumors and its use as an immunodiagnostic marker. *Clinics (Sao Paulo)* 2011;**66**:965−72.
83. Wang J, Ye C, Chen C, Xiong H, Xie B, Zhou J, et al. Glucose transporter GLUT1 expression and clinical outcome in solid tumors: a systematic review and meta-analysis. *Oncotarget* 2017;**8**:16875−86.
84. FDA. *New fludeoxyglucose F18 injection PET drug approved in less than 6 months*. 2014. Available from: https://www.fda.gov/drugs/pharmaceutical-quality-resources/update-new-fludeoxyglucose-f-18-injection-pet-drug-approved-less-6-months.
85. Agrawal A, Rangarajan V. Appropriateness criteria of FDG PET/CT in oncology. *Indian J Radiol Imaging* 2015;**25**:88−101.

86. Chung JH, Cho KJ, Lee SS, Baek HJ, Park JH, Cheon GJ, et al. Overexpression of Glut1 in lymphoid follicles correlates with false-positive ^{18}F-FDG PET results in lung cancer staging. *J Nucl Med* 2004;**45**:999−1003.
87. Bar-Shalom R, Yefremov N, Guralnik L, Gaitini D, Frenkel A, Kuten A, et al. Clinical performance of PET/CT in evaluation of cancer: additional value for diagnostic imaging and patient management. *J Nucl Med* 2003;**44**:1200−9.
88. Horiuchi C, Tsukuda M, Taguchi T, Ishiguro Y, Okudera K, Inoue T. Correlation between FDG-PET findings and GLUT1 expression in salivary gland pleomorphic adenomas. *Ann Nucl Med* 2008;**22**:693−8.
89. Mano Y, Aishima S, Kubo Y, Tanaka Y, Motomura T, Toshima T, et al. Correlation between biological marker expression and fluorine-18 fluorodeoxyglucose uptake in hepatocellular carcinoma. *Am J Clin Pathol* 2014;**142**:391−7.
90. Kitamura K, Hatano E, Higashi T, Narita M, Seo S, Nakamoto Y, et al. Proliferative activity in hepatocellular carcinoma is closely correlated with glucose metabolism but not angiogenesis. *J Hepatol* 2011;**55**:846−57.
91. Higashi T, Saga T, Nakamoto Y, Ishimori T, Mamede MH, Wada M, et al. Relationship between retention index in dual-phase ^{18}F-FDG PET, and hexokinase-II and glucose transporter-1 expression in pancreatic cancer. *J Nucl Med* 2002;**43**:173−80.
92. Kaira K, Endo M, Abe M, Nakagawa K, Ohde Y, Okumura T, et al. Biologic correlation of 2-[^{18}F]-fluoro-2-deoxy-D-glucose uptake on positron emission tomography in thymic epithelial tumors. *J Clin Oncol* 2010;**28**:3746−53.
93. Wang ZG, Yu MM, Han Y, Wu FY, Yang GJ, Li DC, et al. Correlation of Glut-1 and Glut-3 expression with F-18 FDG uptake in pulmonary inflammatory lesions. *Medicine (Baltim)* 2016;**95**:e5462.
94. Hong R, Lim SC. ^{18}F-fluoro-2-deoxyglucose uptake on PET CT and glucose transporter 1 expression in colorectal adenocarcinoma. *World J Gastroenterol* 2012;**18**:168−74.
95. Groheux D, Giacchetti S, Moretti JL, Porcher R, Espie M, Lehmann-Che J, et al. Correlation of high ^{18}F-FDG uptake to clinical, pathological and biological prognostic factors in breast cancer. *Eur J Nucl Med Mol Imaging* 2011;**38**:426−35.
96. Kitajima K, Miyoshi Y. Present and future role of FDG-PET/CT imaging in the management of breast cancer. *Jpn J Radiol* 2016;**34**:167−80.
97. Godoy A, Ulloa V, Rodriguez F, Reinicke K, Yañez AJ, Garcia Mde L, et al. Differential subcellular distribution of glucose transporters GLUT1-6 and GLUT9 in human cancer: ultrastructural localization of GLUT1 and GLUT5 in breast tumor tissues. *J Cell Physiol* 2006;**207**:614−27.
98. Wuest M, Hamann I, Bouvet V, Glubrecht D, Marshall A, Trayner B, et al. Molecular imaging of GLUT1 and GLUT5 in breast cancer: a multitracer positron emission tomography imaging study in mice. *Mol Pharmacol* 2018;**93**:79−89.
99. Warburg O. On the origin of cancer cells. *Science* 1956;**123**:309−14.
100. Kong SC, Nohr-Nielsen A, Zeeberg K, Reshkin SJ, Hoffmann EK, Novak I, et al. Monocarboxylate transporters MCT1 and MCT4 regulate migration and invasion of pancreatic ductal adenocarcinoma cells. *Pancreas* 2016;**45**:1036−47.
101. Pinheiro C, Longatto-Filho A, Azevedo-Silva J, Casal M, Schmitt FC, Baltazar F. Role of monocarboxylate transporters in human cancers: state of the art. *J Bioenerg Biomembr* 2012;**44**:127−39.
102. Baltazar F, Pinheiro C, Morais-Santos F, Azevedo-Silva J, Queiros O, Preto A, et al. Monocarboxylate transporters as targets and mediators in cancer therapy response. *Histol Histopathol* 2014;**29**:1511−24.
103. Kurhanewicz J, Vigneron DB, Ardenkjaer-Larsen JH, Bankson JA, Brindle K, Cunningham CH, et al. Hyperpolarized ^{13}C MRI: path to clinical translation in oncology. *Neoplasia* 2019;**21**:1−16.
104. Jackson VN, Halestrap AP. The kinetics, substrate, and inhibitor specificity of the monocarboxylate (lactate) transporter of rat liver cells determined using the fluorescent intracellular pH indicator, 2′,7′-bis(-carboxyethyl)-5(6)-carboxyfluorescein. *J Biol Chem* 1996;**271**:861−8.
105. Halestrap AP. The SLC16 gene family—structure, role and regulation in health and disease. *Mol Asp Med* 2013;**34**:337−49.
106. Morris ME, Felmlee MA. Overview of the proton-coupled MCT (SLC16A) family of transporters: characterization, function and role in the transport of the drug of abuse gamma-hydroxybutyric acid. *AAPS J* 2008;**10**:311−21.
107. Halestrap AP. The monocarboxylate transporter family—structure and functional characterization. *IUBMB Life* 2012;**64**:1−9.
108. Broer S, Schneider HP, Broer A, Rahman B, Hamprecht B, Deitmer JW. Characterization of the monocarboxylate transporter 1 expressed in *Xenopus laevis* oocytes by changes in cytosolic pH. *Biochem J* 1998;**333**(1):167−74.
109. Manning Fox JE, Meredith D, Halestrap AP. Characterisation of human monocarboxylate transporter 4 substantiates its role in lactic acid efflux from skeletal muscle. *J Physiol* 2000;**529 Pt 2**:285−93.
110. Halestrap AP, Meredith D. The *SLC16* gene family-from monocarboxylate transporters (MCTs) to aromatic amino acid transporters and beyond. *Pflugers Arch* 2004;**447**:619−28.
111. Pullen TJ, Sylow L, Sun G, Halestrap AP, Richter EA, Rutter GA. Overexpression of monocarboxylate transporter-1 (SLC16A1) in mouse pancreatic beta-cells leads to relative hyperinsulinism during exercise. *Diabetes* 2012;**61**:1719−25.
112. He L, Wang H, Zhang Y, Geng L, Yang M, Xu Z, et al. Evaluation of monocarboxylate transporter 4 in inflammatory bowel disease and its potential use as a diagnostic marker. *Dis Markers* 2018;**2018**:2649491.
113. Halestrap AP, Wilson MC. The monocarboxylate transporter family—role and regulation. *IUBMB Life* 2012;**64**:109−19.
114. Sonveaux P, Vegran F, Schroeder T, Wergin MC, Verrax J, Rabbani ZN, et al. Targeting lactate-fueled respiration selectively kills hypoxic tumor cells in mice. *J Clin Investig* 2008;**118**:3930−42.
115. Choi SY, Xue H, Wu R, Fazli L, Lin D, Collins CC, et al. The MCT4 gene: a novel, potential target for therapy of advanced prostate cancer. *Clin Cancer Res* 2016;**22**:2721−33.
116. Payen VL, Hsu MY, Radecke KS, Wyart E, Vazeille T, Bouzin C, et al. Monocarboxylate transporter MCT1 promotes tumor metastasis independently of its activity as a lactate transporter. *Cancer Res* 2017;**77**:5591−601.
117. Faubert B, Li KY, Cai L, Hensley CT, Kim J, Zacharias LG, et al. Lactate metabolism in human lung tumors. *Cell* 2017;**171**:358−371 e9.
118. Latif A, Chadwick AL, Kitson SJ, Gregson HJ, Sivalingam VN, Bolton J, et al. Monocarboxylate transporter 1 (MCT1) is an independent prognostic biomarker in endometrial cancer. *BMC Clin Pathol* 2017;**17**:27.
119. Keshari KR, Sriram R, Koelsch BL, van Criekinge M, Wilson DM, Kurhanewicz J, et al. Hyperpolarized ^{13}C-pyruvate magnetic resonance reveals rapid lactate export in metastatic renal cell carcinomas. *Cancer Res* 2013;**73**:529−38.
120. Sriram R, Gordon J, Baligand C, Ahamed F, Delos Santos J, Qin H, et al. Non-invasive assessment of lactate production and compartmentalization in renal cell carcinomas using hyperpolarized ^{13}C pyruvate MRI. *Cancers (Basel)* 2018;**10**:313.
121. Nelson SJ, Kurhanewicz J, Vigneron DB, Larson PE, Harzstark AL, Ferrone M, et al. Metabolic imaging of patients with prostate cancer using hyperpolarized [1-^{13}C]pyruvate. *Sci Transl Med* 2013;**5**:198ra08.
122. Scroggins BT, Matsuo M, White AO, Saito K, Munasinghe JP, Sourbier C, et al. Hyperpolarized [1-^{13}C]-pyruvate magnetic resonance spectroscopic imaging of prostate cancer *in vivo* predicts efficacy of targeting the warburg effect. *Clin Cancer Res* 2018;**24**:3137−48.
123. Glaudemans AW, Enting RH, Heesters MA, Dierckx RA, van Rheenen RW, Walenkamp AM, et al. Value of ^{11}C-methionine PET in imaging brain tumours and metastases. *Eur J Nucl Med Mol Imaging* 2013;**40**:615−35.
124. Watabe T, Ikeda H, Nagamori S, Wiriyasermkul P, Tanaka Y, Naka S, et al. ^{18}F-FBPA as a tumor-specific probe of L-type amino acid transporter 1 (LAT1): a comparison study with ^{18}F-FDG and ^{11}C-methionine PET. *Eur J Nucl Med Mol Imaging* 2017;**44**:321−31.